A One-Nearest-Neighbor Approach to Identify the Original Time of Infection Using Censored Baboon Sepsis Data*

Li Ang Zhang, BS[1]; Robert S. Parker, PhD[1–4]; David Swigon, PhD[5]; Ipsita Banerjee, PhD[1,3,4]; Soheyl Bahrami, PhD[6]; Heinz Redl, PhD[6]; Gilles Clermont, MD[1–4]

Objectives: Sepsis therapies have proven to be elusive because of the difficulty of translating biologically sound and effective interventions in animal models to humans. A part of this problem originates from the fact that septic patients present at various times after the onset of sepsis, whereas the exact time of infection is controlled in animal models. We sought to determine whether data mining longitudinal physiologic data in a nonhuman primate model of *Escherichia coli*–induced sepsis could help inform the time of onset of infection.

Design: A nearest-neighbor approach was used to back cast the time of onset of infection in animal models of sepsis. Animal data were censored to simulate prospective monitoring at any moment along the septic infection. This was compared against an uncensored database to find the most similar animal in order to estimate the infection onset time. Leave-one-out cross-validation was used for validation. Biomarker selection was performed based on the criteria of estimation accuracy and/or ease of measurement.

Setting: Computational experimental on existing experimental data.

Subjects: Retrospective data from 33 septic baboons (*Papio ursinus*) subjected to *Escherichia coli* infusion. Validation was performed using 14 pigs that were subjected to surgically induced fecal peritonitis and 22 pigs that were subjected to lipopolysaccharide infusion.

Measurements and Main Results: Longitudinal physiologic and serum markers, time of death. The presence of uniquely changing biomarkers during septic infection enabled the estimation of infection onset time in the datasets. Various combinations of temporal biomarkers, such as WBC, oxygen content, mean arterial pressure, and heart rate, yielded estimation accuracies of up to 97.8%. The use of temporal vital signs and a single measurement of serum biomarkers yielded highly accurate estimates without the need for invasive measurements. Validation in the pig data revealed similar results despite the heterogeneity of multiple experimental cohorts. This suggests that the method may be effective if sufficiently similar subjects are present in the database.

Conclusions: One nearest-neighbor analysis showed promise in accurately identifying the onset of infection given a database of known infection times and of sufficient breadth. We suggest that this approach is ready for evaluation within the clinical setting using human data. (*Crit Care Med* 2016; 44:e432–e442)

Key Words: bacterial infection; biomarkers; cluster analysis; data mining; sepsis

***See also p. 1261.**

[1]Department of Chemical and Petroleum Engineering, Swanson School of Engineering, University of Pittsburgh, Pittsburgh, PA.

[2]Clinical Research, Investigation, and Systems Modeling of Acute Illness Laboratory (CRISMA), Department of Critical Care Medicine, University of Pittsburgh, Pittsburgh, PA.

[3]McGowan Institute for Regenerative Medicine, University of Pittsburgh and UPMC, Pittsburgh, PA.

[4]Department of Bioengineering, Swanson School of Engineering, University of Pittsburgh, Pittsburgh, PA.

[5]Department of Mathematics, University of Pittsburgh, Pittsburgh, PA.

[6]Ludwig Boltzmann Institute for Experimental and Clinical Traumatology, AUVA Research Center, Vienna, Austria.

Supplemental digital content is available for this article. Direct URL citations appear in the printed text and are provided in the HTML and PDF versions of this article on the journal's website (http://journals.lww.com/ccmjournal).

Supported, in part, by National Institutes of Health grant R01 GM105728 and by the Department of Education Graduate Assistance in Areas of National Need Fellowship P200A120195.

Mr. Zhang received support for travel from the National Institutes of Health (NIH) (travel to the International Conference for Complex Acute Illness 2014) and received support for this article research from the NIH and the Department of Education. His institution received grant support from the NIH (NIHR01GM105728) and the Department of Education (Graduate Assistance in Areas of National Need Fellowship P200A120195). Dr. Parker received support for this article research from the NIH (R01GM105728) and Department of Education. His institution received grant support from the NIH, Department of Education, and National Science Foundation (NSF). Dr. Swigon received support for this article research from the NIH (R01GM105728) and NSF. His institution received grant support from the NIH and NSF, and he received support for travel from the NIH. Dr. Bahrami has disclosed employment. Dr. Clermont received support for this article research from the NIH (R01GM105728), consulted for Edwards LifeSciences and Astute Medical, and received royalties from UptoDate. His institution received grant support from the NIH and the NSF. The remaining authors have disclosed that they do not have any potential conflicts of interest.

For information regarding this article, E-mail: cler@pitt.edu

DOI: 10.1097/CCM.0000000000001623

Sepsis is a severe acute physiologic response that results from the systemic effects of inflammatory mediators in response to infection. Each year, sepsis afflicts millions worldwide with extensive morbidity and mortality (1). Treatment of sepsis has proven to be a challenge because of the fast-changing dynamics and multiple trajectories and outcomes of the syndrome (2, 3). Progress in sepsis therapeutics has generally been slow. Since 1982, clinical trials for pharmacologic interventions in sepsis showed either no effect or a negative effect on mortality (4). There is currently no Food and Drug Administration–approved drug to treat septic shock. Frustratingly, therapies that have shown promise in animal models have often failed in human trials because of a lack of efficacy or safety concerns (5, 6). Part of this translational disconnect originates from the fact that septic patients are admitted into the hospital at various times after the onset of sepsis symptoms (7, 8). Data collection and treatment initiation are performed relative to the time of enrollment, not to the time of disease onset. Because of the dynamic nature of the physiologic response to infection, both the nature and the timings of potential interventions are likely to be determinant factors in influencing outcome (2, 9). For example, an abrogation of the early tumor necrosis factor response increased mortality in some animal models, whereas most preclinical treatment models showed benefit (10, 11). This may explain, at least in part, why many sepsis therapies that showed promise from animal models, where timing is known, failed in human studies.

Several mathematical and statistical models have been posed to elucidate the fast-acting dynamics of sepsis and to offer predictions regarding the potential effects of interventions and their timing (2, 3, 12, 13). However, training and fitting parameters of these models for individual patients is challenging, in part, due to the aforementioned timing issues with human data collection. For the purposes of such models, a population mean is typically computed from data pooled at time points relative to the time of enrollment. Naive pooling becomes a problem because these data points are located at various points along temporal trajectories of individual patients. Methodological obstacles in developing robust models, such as interindividual timing and variability and response, combined with a lack of familiarity of the research community with such computational tools have delayed the introduction of such advanced tools as core to the design of clinical trials of sepsis.

Identifying the time of onset of infection offers two advantages in human sepsis research. First, it potentially enables the revisiting of previously failed trials with the purpose of analyzing, a posteriori, possible relationships between the elapsed time from onset and effectiveness. Second, identifying onset time enables patient biomarker data to be shifted relative to the time of infection, therefore allowing more effective translation between animal results and human expectations. Furthermore, mathematical models can be properly trained and provide more accurate predictions if mechanistically based, biomarker-driven interventions are contemplated. We present an approach that, at least in three animal models, accurately estimates the time of onset of an inflammatory challenge from commonly obtained measurements.

METHODS

Datasets

A baboon sepsis dataset was retrospectively analyzed for this work (14). The original experimental design was to investigate the therapeutic effects of a nitric oxide synthase (NOS) inhibitor on septic shock. Thirty-three baboons of the species *Papio ursinus* were sedated, and 2×10^9 colony forming units per kilogram of *Escherichia coli* (*E. coli*) were infused IV into each subject over 2 hours. Fluid resuscitation and antibiotic therapy were provided to all subjects throughout the experiment. The proposed NOS inhibitor treatment began after hour 12 on 16 subjects. Animals were treated in accordance with National Institutes of Health guidelines. The experimental protocol was reviewed and approved by the Institutional Animal Care and Use Committee of Biocon Research Laboratories, Pretoria, South Africa. Seventy-three biomarkers were obtained as time series for each baboon, including vital signs, arterial blood gases and lactate, hemodynamic variables, complete blood counts and differential, and biochemistry. Baseline measurements were taken 30 minutes prior to *E. coli* infusion. Additional measurements were collected at specified times throughout the experiment. Subjects that survived the experiment had final measurements taken prior to killing. Biomarkers that were intermittently measured throughout the experiment were eliminated from the analysis. This reduced the number of biomarkers to 29, where measurements were available for all baboons at hours −0.5, 0, 0.5, 1, 2, 3, 4, 5, 6, 11, and 12, where hour 0 marked the beginning of the *E. coli* infusion. This time point was considered the true time of onset of infection. Time points past 12 hours post infection were not used in this analysis. Baboons in the sham and treatment groups were combined for analysis. The biomarkers evaluated herein are listed in **Table 1**.

For validation of the method, two porcine datasets were used. The first dataset included 14 pigs that were subjected to surgically induced peritonitis; of which, seven subjects received a superoxide dismutase treatment. Measurements were collected at 2, 4, 6, 8, 10, and 12 hours after abdominal closure. Both groups were combined during analysis because trajectories between groups were not significantly different. The second dataset included 22 pigs subjected to 1-hour lipopolysaccharide (LPS) infusions: 12 subjects received 1 μg/kg/hr and 10 received 10 μg/kg/hr. Half of the animals received biliverdin. Measurements were collected at 0, 1, 2, 3, 4, 5, and 7 hours after the start of LPS infusion. Despite significant differences in trajectories between LPS doses, all groups were combined during analysis to test the method's performance on a nonhomogenous database. In both porcine studies, baboon-comparable biomarkers were used.

One-Nearest-Neighbor Analysis

Figure 1 provides an illustration of the process to estimate the time of onset of infection for a given subject. The temporal

TABLE 1. Dictionary of Biomarker Acronyms

Acronym	Meaning	Method of Measurement in Baboon Data	Feasibility Within Human Patients
WBC	White blood cell count	Arterial and mixed venous blood sample	M
HR	Heart rate	Straightforward	N
HCO3A	Arterial bicarbonate	Arterial blood gas analysis	M
SVR	Systemic vascular resistance	Arterial catheter	I
HB	Hemoglobin	Arterial and mixed venous blood sample	M
CO	Cardiac output	Thermal-dilution technique with Swan-Ganz catheter	I[a]
CI	Cardiac index	Calculated from CO and body surface area	N
Cco_2	Capillary oxygen content	Calculated from APo_2	I
ABEA	Arterial base excess	Calculated from HCO3A and pHA	M
MAP	Mean arterial blood pressure	Arterial catheter	N[b]
PVR	Pulmonary vascular resistance	Arterial catheter	I
Pao_2	Arterial oxygen tension	Arterial blood gas analysis	M
RBC	Red blood cell count	Arterial and mixed venous blood sample	M
Cao_2	Arterial oxygen content	Calculated from arterial and mixed venous blood sample	I
PLT	Platelet count	Arterial and mixed venous blood sample	M
APo_2	Alveolar oxygen tension	Arterial catheter	M
HCT	Hematocrit	Arterial and mixed venous blood sample	M
PWP	Pulmonary wedge pressure	Pulmonary artery catheter	I
RAP	Central venous pressure	Arterial catheter	I
$Paco_2$	Arterial carbon dioxide tension	Arterial blood gas analysis	M
TEMP	Central blood temperature	Swan-Ganz catheter	N[b]
o_2DEL	Oxygen delivery	Calculated from respirometry and $AaDo_2$	I
$SATAo_2$	Arterial oxygen saturation	Calculated from arterial blood sample	N[b]
MPAP	Mean pulmonary artery pressure	Arterial catheter	I
RR	Respiratory rate	Straightforward	N
HOROW	Horowitz index	Calculated from Pao_2 and fraction of inspired oxygen	M
QUOTIENT	Respiratory quotient	Respirometry	N
pHA	Arterial pH	Arterial blood gas analysis	M
$AaDo_2$	Alveolar-arterial oxygen difference	Calculated from Pao_2 and APo_2	I

N = noninvasive to measure, M = minimally invasive to measure, I = very invasive to measure.

[a]Cardiac output can be estimated via an ultrasound technique, but this technique is not widely adopted.

[b]Widely accepted noninvasive methods exist to obtain or closely estimate this value.

Acronyms used for physiological measurements obtained longitudinally in the animal experiments, the means through which these measurements were obtained, and whether these means are considered invasive, minimally invasive, or noninvasive.

The third column indicates how the biomarker was measured within the baboon data. The right most column indicates the feasibility of measuring the biomarker in patients within a clinical setting.

trajectories of biomarkers for this subject were left censored at all possible time points to simulate prospective monitoring at any given moment along the subject's sepsis trajectory. Trajectories were right censored to 1, 2, 3, or 4 consecutive points to simulate a time period of monitoring. The one-nearest-neighbor method compared the subject's subtrajectory against a database of equal length from the remaining 32 subjects, identified the most similar subtrajectory, and assigned the time of onset as the known time of onset for the most similar subtrajectory.

Suppose a 3-hour WBC data segment was available for a study subject. A Euclidean distance was calculated between this segment and all possible three consecutive WBC points in the database. **Figure 2** conceptualizes this methodology. This

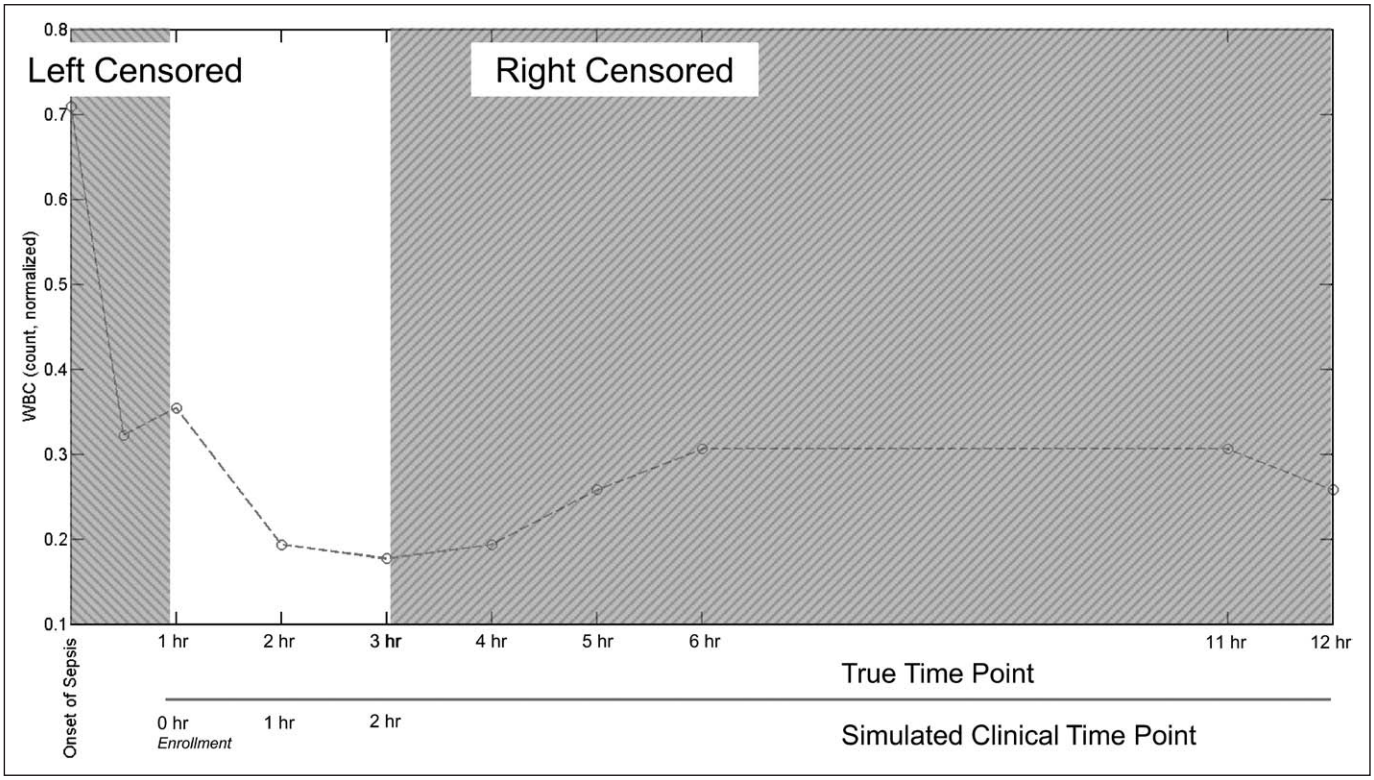

Figure 1. An entire WBC trajectory (normalized to healthy baseline) is shown for a baboon and is censored prior to testing the nearest neighbor method. Left censoring (*left shaded area*) was performed to simulate the passage of time between the onset of sepsis and the first measurement taken at simulated hospital enrollment. All subsequent time points were renumbered to simulate clinical time points where data are relative to hospital enrollment time. Right censoring (*right shaded area*) was performed to emulate sparseness of human data. In this case, measurements ended at 2 hr post enrollment for a total of three subsequent measurements (right censor level 3).

process was repeated for each additional biomarker, and their distances were summed. The 3-hour length subtrajectory in the database with the shortest distance to the study subject's was identified as the nearest neighbor. The first time point of this subtrajectory was used to estimate the study subject's elapsed time since infection. Using more than one nearest neighbor was tested, but it did not improve the accuracy of results (data not shown). A glossary of terms and detailed procedures used are provided in the **supplemental data** (Supplemental Digital Content 1, http://links.lww.com/CCM/B658).

To account for scaling differences across biomarkers and for interbaboon variability, data were normalized on a per-baboon basis. Each subject's biomarker trajectories were normalized to its respective baseline (value at $t = -0.5$ hr prior to infusion). However, the baseline values for the study subject were unknown because of left censoring. A linear regression model for estimating baseline was created for each biomarker using all time points in the database ($\text{biomarker}_{\text{baseline}} = \beta_0 + \beta_1 \times \text{biomarker}_t$). This was used to estimate the unknown baseline values and normalize each biomarker for the study subject. The intercept, β_0, represents a population average baseline, and the slope variable, β_1, represents a subject-specific shift to this baseline.

To test estimation accuracy, we use leave-one-out validation. For each of the 33 subjects, every possible left censoring within the interval (0.5 hr, 12 hr) was tested to emulate a maximum of nine possible "arrival" times. Estimations were generated for each of these cases, and accuracy was determined by dividing the number of correct estimations by the total number of estimations generated. An estimated infection time within a tolerance of ± 1 time point from the actual infection time was deemed correct.

In Silico Experiments

A combinatorial search was performed in order to find the set of biomarkers that yielded the highest accuracy in estimating time of infection while minimizing the number of invasive clinical measurements required. The majority of the 29 biomarkers within the dataset were the result of invasive measurements, and some of these are difficult to collect from human patients. To improve the clinical feasibility of the method, the search was performed involving single-point measurements of minimally invasive biomarkers, that is, blood samples and vital signs.

The first accuracy experiment tested the individual estimation capacity for time of onset of each of the 29 biomarkers across various levels of right censoring. The best biomarkers were identified by calculating the mean accuracy across the four right censoring durations and selecting the top 10. In addition, the null hypothesis was tested by making estimations based on randomly generated trajectories sampled from a zero mean log normal distribution. The second accuracy experiment exhaustively searched all possible combinations of the previously identified top 10 biomarkers. A combinatorial ${}_{10}C_n$ search, where $n \in \{2, 3,..., 10\}$ was performed to identify

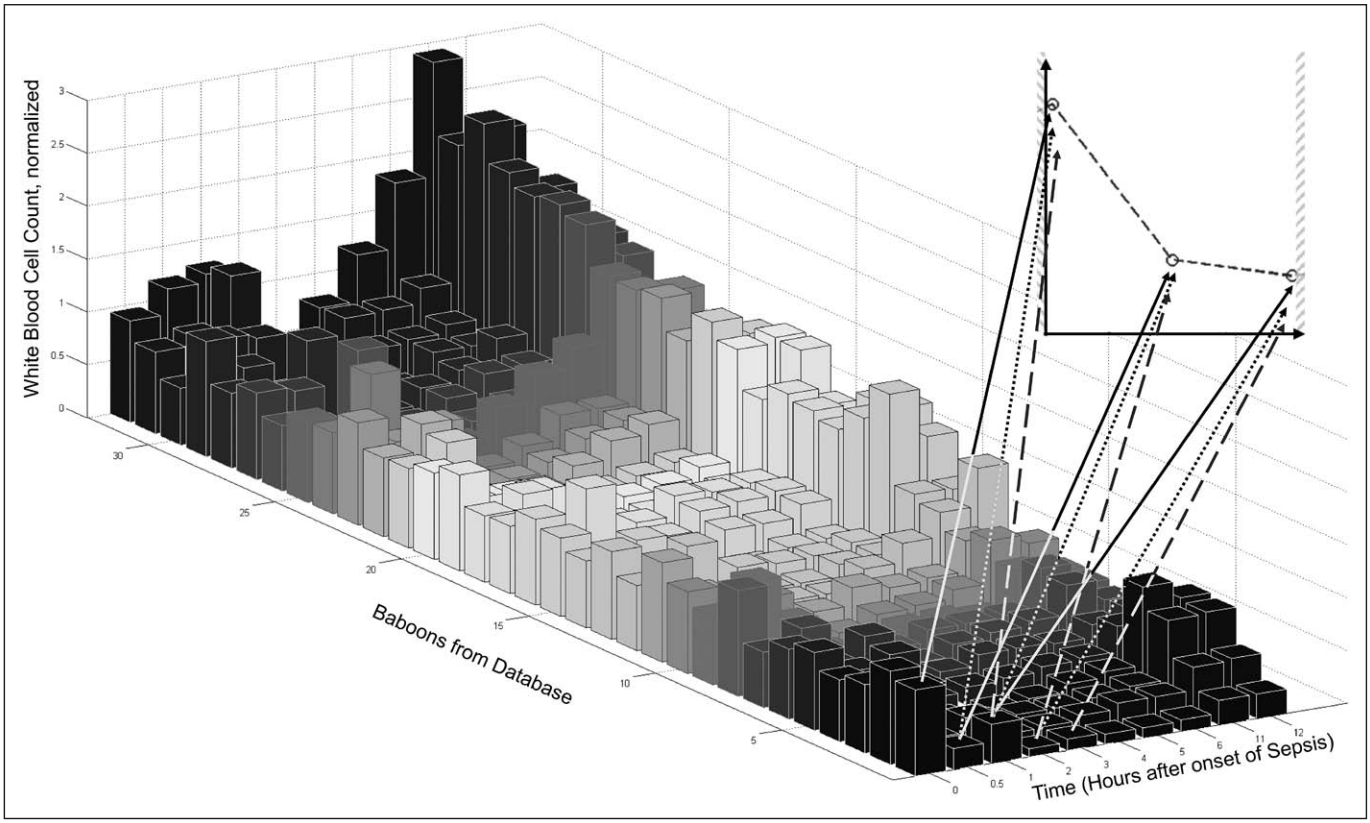

Figure 2. The normalized and censored WBC trajectory from Figure 1 was compared against the WBC database of the remaining 32 baboons (normalized to respective healthy baseline). The 3-point WBC trajectory was compared against every group of three sequential points in the database by calculating a Euclidean distance. Each type of line visualized represents one such comparison. If additional biomarkers were included for analysis, the Euclidean distances from all biomarkers were summed.

the best *n* combinations of biomarkers that identify infection time. This search was performed for each of the right censoring options.

The first feasibility experiment tested the ability of a mixture of time series biomarkers and single-point measure biomarkers to estimate infection time. Vitals heart rate (HR), mean arterial blood pressure (MAP), temperature, arterial oxygen saturation ($SATAO_2$), and respiratory rate (RR) are noninvasive to measure and were made available in time series. Minimally invasive biomarkers WBC, PaO_2, and platelet count (PLT) were chosen because of their diagnostic abilities as listed in the Surviving Sepsis Guidelines (1). In addition, the top three minimally invasive biomarkers from the first accuracy experiment were included as well. All combinations of these vitals and minimally invasive biomarkers were tested for their infection time estimation accuracy. This experiment was repeated for right censoring at 2, 3, and 4 hours. The second feasibility experiment further explored this combination of time series biomarkers and single-point biomarkers by comparing two diagnostic panels that can be realistically performed at the time of patient enrollment. Two minimally invasive diagnostic panels were chosen: arterial blood gas test (yielding arterial base excess, PaO_2, and arterial bicarbonate [HCO3A]) and blood analysis (yielding WBC, PLT, and hemoglobin). Similar to before, vitals were available in time series, and this panel of biomarkers was available at the time of simulated enrollment for a given emulated patient. All combinations of the aforementioned vitals (except for RR) were tested with data from either or both diagnostic panels. RR was excluded because it was not among the top performers in the previous experiment. This experiment was repeated for right censoring at 2, 3, and 4 hours.

For validation, the first accuracy experiment (single-biomarker search) and the first feasibility experiment (vitals + one search) were repeated on each of the pig datasets. The biomarkers used in those experiments were selected to be comparable with those of the baboons.

RESULTS

Accuracy Experiments

Table 2 shows the infection time estimation accuracy of individual biomarkers. The first right censor duration tested only a single-time measurement and yielded low accuracies throughout the table. Accuracy increased as more of the study subject's temporal points were included in the search. Biomarkers were sorted by decreasing mean accuracy across the four right censor durations. WBC was the top biomarker in all columns and yielded a maximum estimation accuracy of 93.1% when using four sequential hourly points. Jackknife resampling of the data revealed that the SD of accuracies across biomarkers and right censor durations had a mean of 0.7%. No entry within Table 2 fell below their respective right censor level null accuracy. The

TABLE 2. Single-Biomarker Prediction Accuracy

	Baboon Accuracy, %					Pig Peritonitis Accuracy, %				Pig Endotoxemia Accuracy, %			
Biomarker	R 1	R 2	R 3	R 4	Mean	R 1	R 2	R 3	Mean	R 1	R 2	R 3	Mean
WBC	51.8	67.0	83.0	93.1	73.7	60.7	58.6	76.8	65.4	46.5	64.4	73.4	61.4
Heart rate	42.1	58.2	74.6	84.8	65.0	64.6	83.8	87.0	78.5	47.2	61.0	69.1	59.1
Arterial bicarbonate	48.5	56.2	67.8	75.3	62.0	–	–	–	–	–	–	–	–
Systemic vascular resistance	32.7	59.3	72.0	79.7	60.9	50.0	57.4	63.0	56.8	50.7	63.6	66.0	60.1
Hemoglobin	34.8	58.2	70.8	79.2	60.8	53.6	67.1	83.9	68.2	52.8	73.7	84.0	70.2
Cardiac output	33.6	54.5	68.9	84.8	60.5	46.3	51.5	64.8	54.2	45.8	55.1	63.8	54.9
Cardiac index	32.1	51.9	72.0	84.4	60.1	–	–	–	–	–	–	–	–
Capillary oxygen content	33.9	55.9	70.8	79.7	60.1	–	–	–	–	–	–	–	–
Arterial base excess	44.8	51.5	65.9	74.5	59.2	59.8	73.5	77.8	70.4	50.4	63.9	69.6	61.3
Mean arterial blood pressure	33.0	50.8	65.9	82.7	58.1	43.9	50.0	61.1	51.7	53.5	65.3	77.7	65.5
Pulmonary vascular resistance	38.5	52.5	66.7	74.5	58.0	–	–	–	–	–	–	–	–
Pao_2	45.2	49.5	63.6	70.6	57.2	53.7	51.5	64.8	56.6	47.2	49.2	61.7	52.7
RBC	29.7	49.8	67.4	78.8	56.4	52.4	74.3	87.5	71.4	54.2	73.7	83.0	70.3
Arterial oxygen content	30.9	51.2	64.0	77.1	55.8	51.2	50.0	57.4	52.9	47.9	56.8	57.4	54.0
Platelet count	50.9	49.2	56.1	60.6	54.2	61.9	70.0	82.1	71.3	41.5	50.0	61.7	51.1
Alveolar oxygen tension	40.3	49.5	56.4	62.8	52.3	–	–	–	–	–	–	–	–
Hematocrit	28.8	45.5	62.9	70.1	51.8	53.6	72.9	91.1	72.5	50.0	65.3	81.9	65.7
Pulmonary occlusion pressure	34.5	53.2	54.2	63.6	51.4	45.1	64.7	81.5	63.8	38.0	46.6	66.0	50.2
Central venous pressure	28.8	46.5	58.7	70.6	51.1	43.9	63.2	70.4	59.2	41.5	51.7	64.9	52.7
$Paco_2$	39.4	52.2	51.5	61.0	51.0	51.2	50.0	57.4	52.9	47.9	56.8	57.4	54.0
Temperature	32.7	49.8	56.1	62.8	50.3	54.9	67.6	83.3	68.6	59.9	66.1	79.8	68.6
Oxygen delivery	31.8	41.4	54.5	73.6	50.3	–	–	–	–	–	–	–	–
Arterial oxygen saturation	34.5	45.8	53.8	62.8	49.2	62.2	58.8	70.4	63.8	55.6	55.9	73.4	61.7
Mean pulmonary artery pressure	37.0	43.8	48.9	58.0	46.9	59.8	52.9	61.1	57.9	47.2	57.6	85.1	63.3
Respiratory rate	29.1	35.4	45.5	59.3	42.3	50.0	73.5	77.8	67.1	36.6	44.1	53.20	44.6
Horowitz index	28.2	38.0	47.3	54.1	41.9	52.44	61.8	72.22	62.14	–	–	–	–
Respiratory quotient	28.2	36.0	43.6	53.7	40.4	–	–	–	–	–	–	–	–
Arterial pH	27.9	38.7	44.3	48.1	39.7	42.7	57.4	75.9	58.7	55.6	65.3	76.6	65.8
Alveolar-arterial oxygen difference	27.6	32.3	45.1	51.5	39.1	–	–	–	–	–	–	–	–
Mean null	26.6	29.0	32.3	36.7	31.2	38.1	44.7	55.0	45.9	42.7	49.1	57.7	49.8

R1 = single measurement, R2 = consecutive measurement, R3 = 3 consecutive measurements, R4 = 4 consecutive measurements.

Time-of-infection estimation accuracy over varying right censor values (temporal durations). Results were generated with available biomarkers from the baboon data and then sorted by mean accuracy. The null hypothesis, tested with randomized biomarkers, performed worse than all of the tested biomarkers. This method was repeated on the two porcine datasets for validation. Only three right censor durations were tested because of the sampling rate and duration limitations of those experiments.

Dashes indicate measurements not available in porcine experiments.

mean null hypothesis accuracy increased with higher right censor levels because of the shrinking of estimation possibilities.

All possible combinations of the top 10 biomarkers from Table 2 were tested to maximize the accuracy at each level of right censorship. The top result for each right censor level is shown in **Table 3**. Remarkably, single-time point measurements of six biomarkers yielded roughly 70% estimation accuracy. WBC was selected in all cases. There was a strong preference given to arterial blood gas measurements, hemoglobin, and cardiovascular measurements.

Feasibility Experiments

The goal of the feasibility experiments was to identify a parsimonious set of biomarkers, in both time series and single-point measurements, which were minimally invasive to measure in humans and yielded a good accuracy in their ability to estimate the time of infection onset. HCO3A, hemoglobin, and cardiac output (CO) were the top performing minimally invasive biomarkers in Table 2 and were included in the experiment. **Table 4** shows the best results from each measurement collection (one minimally invasive biomarker plus a combination of vitals in time series) organized by right censor duration. For comparison, accuracies were calculated for each entry with vitals alone and with all biomarkers in time series. The inclusion of a point measurement had the greatest impact on accuracy for the lower right censor durations. A single value of WBC combined with 2 hours of HR data improved accuracy from 58.2% to 71.4%. HCO3A and WBC were consistently selected throughout the table. Point measures of biomarkers helped many entries achieve over 90% estimation accuracy.

Time series of invasive measurements did not improve accuracy, thus not warranting the extra probing of subjects. For example, two measurements of HR and WBC yielded an estimation accuracy of 81.1%. The same accuracy was achieved by using two measurements of MAP and HR along with a single measurement of HCO3A. Furthermore, the use of MAP, $SATAo_2$, and HR + 1× HCO3A outperformed the majority of entries in each right censor category.

The second feasibility experiment tested the accuracy of using multiple single-point biomarkers with time series vitals. The top three results from the combinatorial search are shown in **Table 5** with results sorted based on accuracies from the "both panels'" column. The information gained by administering both diagnostic panels aided in almost all entries of the 2- and 3-time point right censor levels, achieving maximum accuracies of 84.2% and 90.2%, respectively. Regardless, despite the added data from the diagnostic panels, many entries from Table 4 using a point biomarker yielded equal or higher accuracies.

Method Validation on Porcine Datasets

Table 2 shows single-biomarker accuracies for both pig experiments. Accuracies were, in general, equivalent or higher than those of the baboons. Time of onset estimation differed slightly among the models. For example, hemoglobin, temperature, and hematocrit performed better in both of the pig datasets. Alternatively, PLT performed similarly between the baboon and the pig LPS data but was more informative in the pig peritonitis data. This may be the result of the differences in sepsis induction protocols across the three models and suggestive toward the existence of sepsis endotypes characterized by distinctive biomarker trajectories.

The vitals + one biomarker search on the porcine data revealed MAP, temperature, and $SATAo_2$ to provide highly accurate estimates (LPS: 70–90+%; peritonitis: 80–90+%) when used in conjunction with a single WBC or arterial pH measurement. Detailed porcine results from this search are available in **Supplemental Tables 1** and **2** (Supplemental Digital Content 1, http://links.lww.com/CCM/B658).

DISCUSSION

A one-nearest-neighbor approach was selected to tackle the problem of identifying infection time from left and right censored data. We found that serial measurements of noninvasive vital signs, combined with a single minimally invasive, yet routinely done, blood work, yielded good accuracy to identify time of onset of infection in an experimental baboon model of sepsis. The method was further confirmed in two additional animal models. The one-nearest-neighbor method was developed based on the hypothesis that cohorts of septic subjects exist with similar characteristic biologic responses. The baboon

TABLE 3. Multiple Biomarker Prediction Accuracy

Right Censor Length	Biomarkers	Accuracy, %		
		Baboon	Pig Peritonitis	Pig Lipopolysaccharide
1 time point	WBC, HCO3A, HR, SVR, CI, and arterial base excess	72.7	71.9	58.9
2 time points	WBC, HCO3A, MAP, HB, CO, and Cco_2	85.9	70.6	72.4
3 time points	WBC, HR, HCO3A, MAP, SVR, and HB	93.2	87.0	93.5
4 time points	WBC, HR, MAP, CO, Cco_2 HCO3A, HB, and CI	97.8	–	–

HCO3A = arterial bicarbonate, HR = heart rate, SVR = systemic vascular resistance, CI = cardiac index, MAP = mean arterial blood pressure, HB = hemoglobin, CO = cardiac output, Cco_2 = capillary oxygen content.

All possible *n* biomarker combinations of the top 10 (baboon) biomarkers from Table 2 were tested for their predictive accuracy. The best biomarker set is shown for each right censor duration under baboon accuracy. Validation of these biomarkers were performed on the porcine datasets. Arterial bicarbonate, cardiac index, and capillary oxygen content were unavailable for the porcine datasets and were respectively substituted by pH, cardiac output, and Pao_2.

Dashes indicate measurements not available in porcine experiments.

TABLE 4. Prediction Accuracy of Longitudinal Vital Signs With a Single Blood Biomarker

Right Censor	Time Series Biomarkers	Point Biomarker	Accuracy, %		
			No Point	With Point	Time Series Point
2 time points	HR	WBC	58.2	71.4	81.1
	HR	HCO3A	58.2	70.0	71.7
	MAP	HCO3A	50.8	69.4	70.0
	MAP and HR	HCO3A	70.0	81.1	81.1
	MAP and HR	WBC	70.0	77.8	81.1
	$SATAo_2$ and HR	WBC	60.3	76.1	81.8
	MAP, $SATAo_2$, and HR	HCO3A	76.8	81.8	81.5
	TEMP, MAP, and HR	HCO3A	73.4	81.1	81.1
	TEMP, MAP, and HR	Pao_2	73.4	79.1	81.1
	TEMP, MAP, $SATAo_2$, and HR	HCO3A	75.4	81.8	81.8
	TEMP, MAP, $SATAo_2$, and HR	WBC	75.4	80.1	82.2
	TEMP, MAP, $SATAo_2$, and HR	Pao_2	75.4	80.1	81.8
3 time points	HR	WBC	74.6	76.9	86.4
	MAP	HCO3A	65.9	75.8	81.8
	HR	HCO3A	74.6	75.4	78.4
	MAP and HR	HCO3A	87.5	89.8	92.0
	MAP and HR	HB	87.5	89.0	90.5
	MAP and HR	Pao_2	87.5	88.3	92.8
	MAP, $SATAo_2$, and HR	HCO3A	88.3	92.0	92.8
	MAP, $SATAo_2$, and HR	Pao_2	88.3	91.3	93.9
	MAP, $SATAo_2$, and HR	HB	88.3	89.4	91.7
	TEMP, MAP, $SATAo_2$, and HR	HCO3A	87.5	92.0	92.8
	TEMP, MAP, $SATAo_2$, and HR	Pao_2	87.5	90.5	93.9
	TEMP, MAP, $SATAo_2$, and HR	HB	87.5	89.4	91.3
4 time points	MAP	HCO3A	82.7	88.3	89.2
	MAP	WBC	82.7	86.1	94.4
	HR	HCO3A	84.8	85.7	88.7
	MAP and HR	WBC	94.4	94.8	94.4
	MAP and HR	HCO3A	94.4	94.8	95.2
	MAP and HR	HB	94.4	93.9	94.4
	MAP, $SATAo_2$, and HR	HCO3A	95.2	96.1	96.5
	TEMP, MAP, and HR	WBC	93.9	95.2	93.9
	MAP, $SATAo_2$, and HR	WBC	95.2	95.2	94.8
	TEMP, MAP, $SATAo_2$, and HR	WBC	95.7	95.2	94.8
	TEMP, MAP, $SATAo_2$, and HR	HCO3A	95.7	95.2	96.5
	TEMP, MAP, $SATAo_2$, and HR	Pao_2	95.7	95.2	97.0

HR = heart rate, HCO3A = arterial bicarbonate, MAP = mean arterial blood pressure, $SATAo_2$ = arterial oxygen saturation, TEMP = temperature, HB = hemoglobin.

Results from the first feasibility experiment where vital signs in time series were combined with single-point measurements (at the time of simulated enrollment) of minimally invasive biomarkers to estimate infection time. Vitals temperature, mean arterial blood pressure, arterial oxygen saturation, heart rate, respiratory rate, or in any combination thereof, was tested in conjunction with a single blood biomarker for their prediction accuracy. The top three biomarker sets for each combination and right censor duration are shown, with their accuracies listed in the "with point" column. "No point" shows the estimation accuracy for the vitals without the point biomarker. "Time series point" shows the estimation accuracy when all biomarkers (vitals and point) were available in time series.

TABLE 5. Prediction Accuracy of Longitudinal Vitals With Different Diagnostic Blood Panels

Right Censor	Time Series Biomarkers	Accuracy, %		
		Both Panels' Accuracy	Blood Cell Panel Accuracy	Arterial Blood Gas Panel Accuracy
2 time points	MAP	81.8	74.7	69.0
	HR	79.5	71.0	70.4
	TEMP	77.4	65.0	58.3
	MAP and HR	82.2	78.8	78.8
	MAP and $SATAo_2$	77.8	76.1	70.0
	TEMP and MAP	77.4	76.1	70.0
	TEMP, MAP, and HR	82.8	79.8	78.5
	MAP, $SATAo_2$, and HR	82.2	80.5	78.5
	TEMP, MAP, and $SATAo_2$	77.8	77.1	69.7
	TEMP, MAP, $SATAo_2$, and HR	84.2	81.1	77.8
3 time points	MAP	86.7	77.7	75.8
	HR	85.6	70.5	75.4
	TEMP	81.1	62.2	54.9
	MAP and HR	83.7	84.5	84.5
	TEMP and MAP	79.9	78.4	75.8
	MAP and $SATAo_2$	79.6	80.7	76.9
	TEMP, MAP, and HR	83.7	85.2	84.8
	MAP, $SATAo_2$, and HR	83.7	86.0	85.2
	TEMP, MAP, and $SATAo_2$	80.7	80.3	77.3
	TEMP, MAP, $SATAo_2$, and HR	90.2	86.7	85.2
4 time points	MAP	90.5	84.8	81.8
	HR	89.2	80.5	78.8
	$SATAo_2$	87.5	68.4	64.5
	MAP and HR	89.6	95.2	88.7
	MAP and $SATAo_2$	87.0	87.0	83.5
	TEMP and MAP	86.2	85.3	82.7
	TEMP, MAP, and HR	90.0	94.8	89.6
	MAP, $SATAo_2$, and HR	89.6	95.7	90.9
	TEMP, MAP, and $SATAo_2$	87.5	87.0	83.5
	TEMP, MAP, $SATAo_2$, and HR	93.5	95.2	90.9

MAP = mean arterial blood pressure, HR = heart rate, TEMP = temperature, $SATAo_2$ = arterial oxygen saturation.

Results from the comparison of two types of diagnostic panels: arterial blood gas (arterial bicarbonate, Pao_2, and arterial base excess) and blood analysis (WBC, platelet count and hemoglobin). Vitals temperature, mean arterial blood pressure, arterial oxygen saturation, heart rate, or in any combination thereof were tested in conjunction with either or both diagnostic panels for their estimation accuracy. The top performing combinations are shown.

study chosen for analysis represented a homogenous cohort that all exhibited leukopenia following the *E. coli* infusion. Pig validation sets did not share this feature. Given a censored and normalized trajectory for a study baboon, one-nearest-neighbor identified the most similar trajectory within the database. The temporal information of this trajectory provided the time-of-infection estimate for the study baboon. To the best of our knowledge, there are currently no proposed methods to identify time of onset of an inflammatory challenge for sepsis or nonsepsis data. A related article was found to use a variable

k-nearest-neighbor approach for the purposes of early diagnosis in neonatal sepsis (15). Another recent article used the nearest-neighbor approach to identify novel genes associated with sepsis severity (16). Nearest-neighbor approach is a popular nonparametric approach in data mining and was selected here to find similarities among biomarker trajectories.

The exhaustive biomarker search revealed that certain biomarkers provide highly accurate estimations of time of onset of infection. WBC, HR, hemoglobin, MAP, and HCO3A were the top performers in Table 2 and had many appearances in Table 3. In contrast to CO or systemic vascular resistance (SVR), both of which require the insertion of an arterial catheter, WBC, HR, hemoglobin, MAP, and HCO3A are relatively easy to measure. The modest accuracy increase from the inclusion of CO or SVR is of doubtful clinical significance and did not seem to justify the invasive measurement. This suggested that more invasive-to-measure biomarkers might be unnecessary and that this time of infection onset can be estimated with easily measured, patient-friendly biomarkers. It is also interesting to note the consistent appearance of many biomarkers across animal models.

Most clinicians do not perform consecutive hourly blood sample tests, and only noninvasive biomarkers are likely to be acquired in time series. Many biomarkers in the baboon data cannot be obtained hourly (or ever) in human patients because of practical reasons (no available commercial assay, slow turnovers) or to unjustifiable expenses. Patients with suspected sepsis upon enrollment sometimes have a panel of diagnostic tests administered, including arterial blood gas tests and a WBC measurement. These measurements are typically only taken once at the time of enrollment. In contrast, vital signs such as HR, MAP, temperature, and $SATAO_2$ are continuously monitored and universally measured in time series. The feasibility experiments addressed these issues by using clinically obtainable data from humans and yielded interesting results. Specifically, they showed that 1) the addition of a minimally invasive point measurement generally improved time-of-infection accuracy over the use of time series vitals alone, 2) taking minimally invasive measurements in time series may be unnecessary for estimating time-of-infection, and 3) there existed a data saturation limit where one-nearest-neighbor did not benefit from additional data.

The main limitation associated with this method was the small sample size of all three datasets. This method worked well for the heterogeneous pig datasets at least, in part, because of the uniformity of the insult within datasets, thus improving the chances of a relevant "closest looking" animal in the cohort. If the database does not contain sufficiently similar subjects to an incoming subject for which an estimation is to be made, the method might not be able to generate a meaningful estimate.

Three main challenges currently prevent this method from being directly translated to human patients. First, developing a human model requires access to a temporally rich collection of physiologic markers at baseline and following time of infection. The second challenge is human variability, demanding that the dataset be of sufficient size to be representative on most endotypes. Third, human sepsis often happens in conjunction with other inflammatory stressors, such as surgery or trauma. To address these challenges, a human dataset of sufficient breadth could potentially be assembled in a cohort of patients developing sepsis in association with an invasive procedure, therefore bounding time of onset to within a few hours. The impact of the procedure itself on biomarker time series would constitute useful additional information.

Although human patients exhibit high variability, we argue that there exists a finite number of sepsis endotypes and that these endotypes can be grouped into cohorts with similar clinical biomarker trajectories. Future work will employ data-mining techniques to classify these endotypes and to identify the associated biomarkers. By informing a nearest-neighbor search on a sufficiently varied database with endotype-indicative biomarkers, the method should have enough discrimination to generate meaningful estimates of sepsis onset times.

CONCLUSIONS

We propose a novel application of the nearest-neighbor approach to estimate the onset time of infection within artificially censored baboon and porcine sepsis data. High accuracies were achieved with varying sets of biomarkers, but some biomarkers are difficult to measure clinically in humans. A compromise was made between minimizing the invasiveness of measurement and maximizing the estimation accuracy. A feasible set of clinically measurable biomarkers was identified; combinations of vital signs in time series and minimally invasive point measurements yielded similar but slightly lower accuracies.

There are no other approaches to estimating time of -infection in sepsis, and the method developed here may have profound implications if successfully extended for use with human data. Septic patients would be able to be grouped into early, middle, and late infection times and treated differently, which may play a clinically meaningful role in patient outcomes. Clinical trials may be revisited or new therapeutic targets may emerge because treatment timings can be more effectively controlled with respect to the temporal span of infection. Finally, computational models of sepsis and immunomodulatory interventions used in the design of such trials may immediately benefit from the knowledge of infection times.

REFERENCES

1. Dellinger RP, Levy MM, Rhodes A, et al; Surviving Sepsis Campaign Guidelines Committee including the Pediatric Subgroup: Surviving sepsis campaign: International guidelines for management of severe sepsis and septic shock: 2012. *Crit Care Med* 2013; 41:580–637
2. Kumar R, Clermont G, Vodovotz Y, et al: The dynamics of acute inflammation. *J Theor Biol* 2004; 230:145–155
3. Reynolds A, Rubin J, Clermont G, et al: A reduced mathematical model of the acute inflammatory response: I. Derivation of model and analysis of anti-inflammation. *J Theor Biol* 2006; 242:220–236
4. Fink MP: Animal models of sepsis. *Virulence* 2014; 81:137–43
5. Rittirsch D, Hoesel LM, Ward PA: The disconnect between animal models of sepsis and human sepsis. *J Leukoc Biol* 2007; 81: 137–143

6. Suntharalingam G, Perry MR, Ward S, et al: Cytokine storm in a phase 1 trial of the anti-CD28 monoclonal antibody TGN1412. *N Engl J Med* 2006; 355:1018–1028
7. Rivers EP, Jaehne AK, Nguyen HB, et al: Early biomarker activity in severe sepsis and septic shock and a contemporary review of immunotherapy trials: Not a time to give up, but to give it earlier. *Shock* 2013; 39:127–137
8. Puskarich MA, Trzeciak S, Shapiro NI, et al; Emergency Medicine Shock Research Network (EMSHOCKNET): Association between timing of antibiotic administration and mortality from septic shock in patients treated with a quantitative resuscitation protocol. *Crit Care Med* 2011; 39:2066–2071
9. Cross AS, Opal SM: A new paradigm for the treatment of sepsis: Is it time to consider combination therapy? *Ann Intern Med* 2003; 138:502–505
10. Moore TA, Perry ML, Getsoian AG, et al: Increased mortality and dysregulated cytokine production in tumor necrosis factor receptor 1-deficient mice following systemic *Klebsiella pneumoniae* infection. *Infect Immun* 2003; 71:4891–4900
11. Bodmer M, Fournel MA, Hinshaw LB: Preclinical review of anti-tumor necrosis factor monoclonal antibodies. *Crit Care Med* 1993; 21:S441–S446
12. DiLeo MV, Kellum JA, Federspiel WJ: A simple mathematical model of cytokine capture using a hemoadsorption device. *Ann Biomed Eng* 2009; 37:222–229
13. Day J, Rubin J, Vodovotz Y, et al: A reduced mathematical model of the acute inflammatory response II. Capturing scenarios of repeated endotoxin administration. *J Theor Biol* 2006; 242:237–256
14. Schlag G, Redl H (Eds): Shock, Sepsis, and Organ Failure. Berlin, Heidelberg, Springer Berlin Heidelberg, 1999
15. Xiao Y, Griffin MP, Lake DE, et al: Nearest-neighbor and logistic regression analyses of clinical and heart rate characteristics in the early diagnosis of neonatal sepsis. *Med Decis Making* 2010; 30:258–266
16. Khaenam P, Rinchai D, Altman MC, et al: A transcriptomic reporter assay employing neutrophils to measure immunogenic activity of septic patients' plasma. *J Transl Med* 2014; 12:65